Electronic Supplementary Material (ESI) for Analyst.

Supporting Information

DNA Nanodevices Monitored with Fluorogenic Looped-Out 2-Aminopurine

Pai Peng, Yi Du and Tao Li*

Department of Chemistry, University of Science and Technology of China, 96 Jinzhai Road, Hefei, Anhui 230026 (China); E-mail: tlitao@ustc.edu.cn

Table of Contents

Ⅰ. Supplementary figures and discussion

Fluorescence quantum yield test

Fluorescence quantum yields were determined by using the reported equation[1]:

$$\Phi = \Phi_{ref} \frac{\int I(\lambda) d\lambda A_{ref}}{I_{ref}(\lambda) d\lambda \ A}$$

Quinine sulfate was prepared in 0.05 M H_2SO_4 and used as a reference for fluorescence quantum yield measurement. In this equation, Φ_{ref} refers to 0.55, the standard quantum yield of quinine sulfate. $I(\lambda)$ refers to the fluorescence intensity. A refers to the UV absorbance at the excited wavelength. To remove the interference of pure DNA in absorbance, it is subtracted from the absorbance of 2-AP at 310 nm.[2]

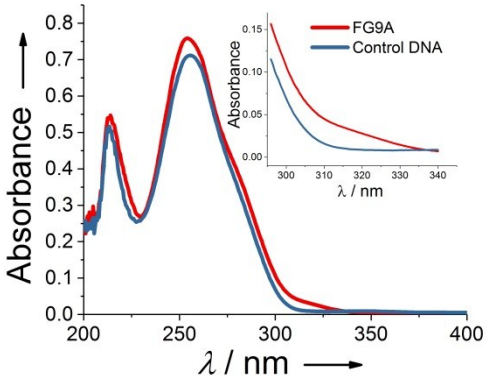

Figure S1. Absorption spectra of FG9A and the control G-quadruplex DNA (using adenine to replace 2-AP) in the presence of K^+. The two DNA G-quadruplexes both adopt parallel structures.

Table S1. Fluorescence quantum yields of 2-AP in different DNA structures, together with those of TAMRA, Cy3 and fluorescein obtained from the references 3–5.

Single strand	0.0167
Double strand	0.0182
1-Base loop (Duplex)	0.3385
2-Base loop (Duplex)	0.0577
3-Base loop (Duplex)	0.0972
1-Base loop (Triplex)	0.5068
2-Base loop (Triplex)	0.1724
3-Base loop (Triplex)	0.0625
Parallel folded FG9A	0.5978
Antiparallel folded FG9A	0.0028
TAMRA (internally labeled)[3]	0.53
Cy3 (internally labeled)[4]	0.21
Fluorescein[5]	0.440

Molar extinction coefficient

The product of quantum yield and molar extinction coefficients together reflect the signal intensity of fluorophores. Therefore, we compared the extinction coefficient of 2-AP and the other fluorophores on the basis of reported references. The acquirable signal of 2-AP is weaker than those of TAMRA, Cy3 or fluorescein.

Table S2. Reported fluorescence extinction coefficients of 2-AP, TAMRA, Cy3.

Fluorophore name	Extinction coefficient ($L*mol^{-1}*cm^{-1}$)
2-AP[6]	10,000
TAMRA[7]	90,000
Cy3[8]	150,000
Fluorescein[9]	78,000

Two patterns for splitting fluorogenic parallel G-quadruplexes

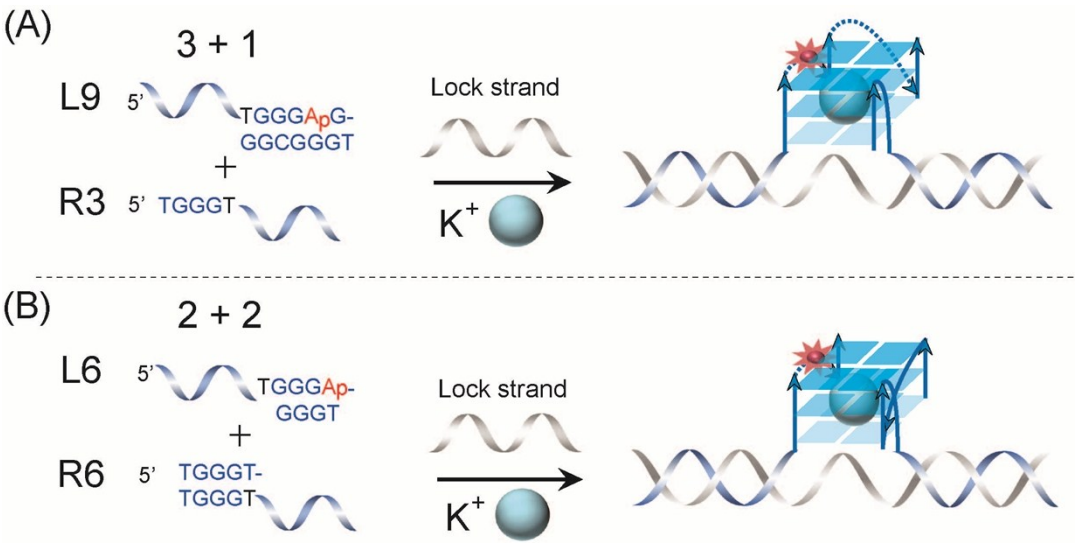

Figure S2. Two patterns of fluorogenic split G-quadruplex including (A) 3+1 G-tracts/L9R3 and (B) 2+2 G-tracts/L6R6 in the presecnce of "lock strand" and potassium ions.

Performance of the two patterns of split parallel G-quadruplexes

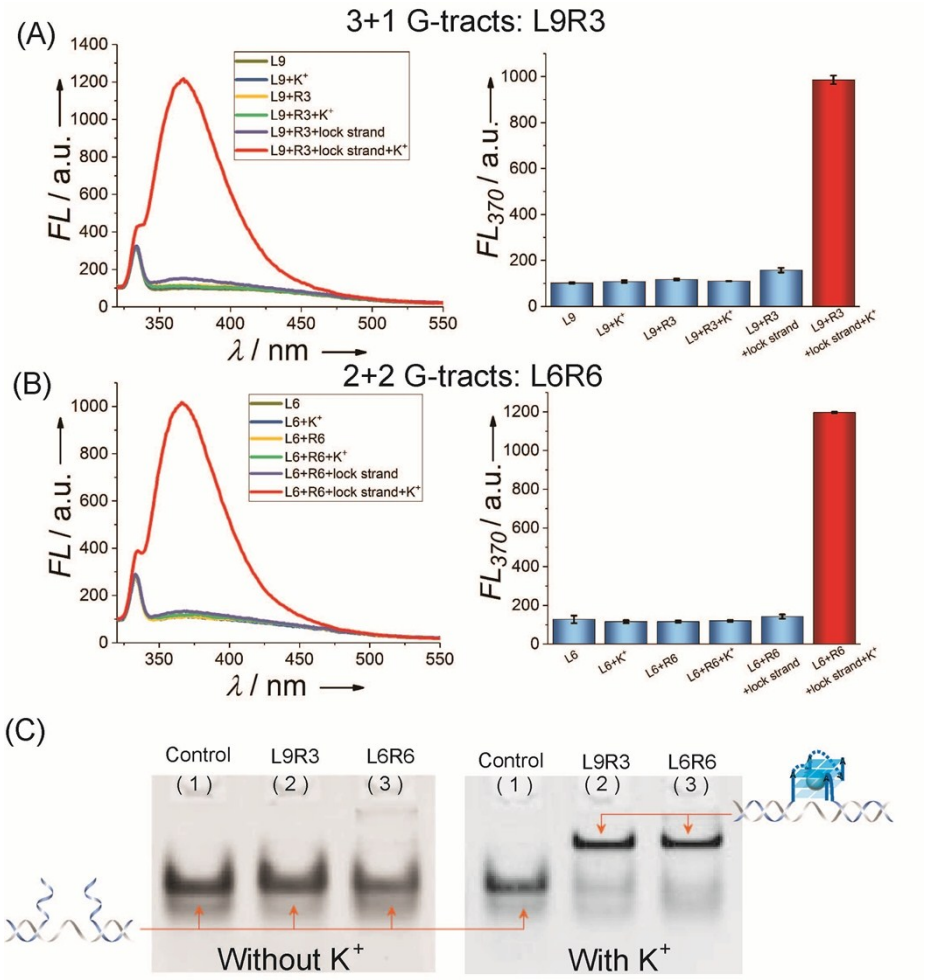

Figure S3. Fluorescence spectra and the corresponding bar representations of the forming process of (A) L9R3/ the 3+1 split G-quadruplex and (B) L6R6/ the 2+2 split G-quadruplex. (C) Gel electrophoretograms of L9R3 and L6R6 in the absence and presence of K^+.

We explored the fluorescence performance of 2-AP in the two split patterns by tethering the two components to the ends of two single strands, respectively (Figure S2). The "lock strand" is an antisense strand for the non-G-rich regions of these two G-tracts incorporated single strands, drawing the guanine residues nearer. In the absence of potassium ions, the two G-rich residues cannot come in contact to each other and 2-AP shows weak fluorescence in this case. In contrast, they come nearer and are folded into parallel G-quadruplexes stabilized by potassium ions. Meanwhile, 2-AP is looped-out in the double-chain-reversal loop, which displays high fluorescence.

Figure S3A and S3B depicts the fluorescence behaviours of 2-AP through the forming process of the fluorogenic split G-quadruplexes. Both for the two split patterns, the split parallel G-quadruplexes are formed when the two G-rich split strands, "lock strands" and potassium ions coexist in solutions. The fluorescence of 2-AP increased dramatically only when all of them are present at the same time, revealing that the fluorogenic split G-quadruplexes are formed whereas lacking any constituent part of them leads to

weak fluorescence. Experimental results indicate that 2-AP in the two split patterns shows approximately the same fluorescence performance.

Moreover, the validity of the two patterns for splitting parallel G-quadruplexes was further confirmed by native PAGE (Figure S3C). L9R3 and L6R6 (lane 2 and lane 3) display the same electrophoretic mobility with or without K^+, indicating that G-quadruplexes in the two split patterns adopt similar conformations. Whereas they move much slower than the reference bands (lane 1, the non-G-quadruplex structure with the same number of bases as split G-quadruplexes) in the presence of K^+, due to the increasing steric hinderance of the larger volume sizes of formed split parallel G-quadruplexes. This structural transformations in the presence of K^+ confirmed the effectiveness of our designed two split patterns of fluorogenic G-quadruplexes.

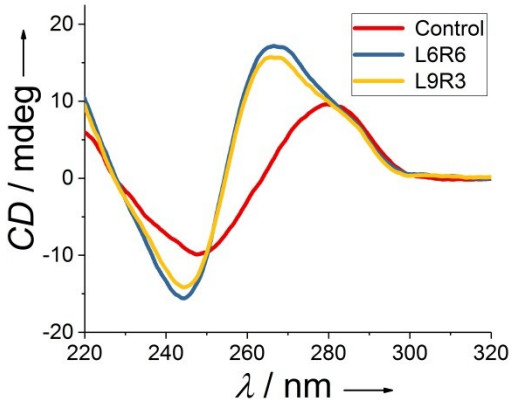

Figure S4. CD spectra of the parallel G-quadruplexes in two split patterns (L6R6 and L9R3) in the presence of K^+.

Meanwhile, circular dichroism spectra (Figure S4) of the split G-quadruplexes in two patterns display a typical CD spectral characteristic of parallel G-quadruplexes,[10] with a positive peak near 265 nm and a negative peak near 245 nm, which verified the parallel folding topologies of the split G-quadruplexes.

Effects of serum concentrations on the fluorescence of 2-AP

We further investigated the effects of serum on the fluorescence of 2-AP. It is reported that proteins in serum show high fluorescence around 360 nm,[11, 12] which overlaps the fluorescence emission spectra of 2-AP. We designed a looped-out 2-AP-incorportated duplex, and studied the fluorescence of 2-AP in single strand and looped-out double strand. In Figure S5, it is observable that the fluorescence of proteins increases with ascending serum concentrations. To overcome this, we deducted the background fluorescence of serum from that of 2-AP and utilized the fluorescence change (ΔFL) to assess the efficiency of looped-out 2-AP (Figure S5B–S5E). It is easy to see that the maximum fluorescence intensity of looped-out 2-AP decreases gradually when the serum concentrations increases. Meanwhile, the fluorescence intensity of 2-AP in single strand increases. This phenomenon might come from the protein adsorption effect toward DNA strands, which passivates the DNA interactions. Taking these into consideration, we performed the FL-HCR process in 10% serum (Figure 5C). Results show that the fluorescence increases with increasing HBV gene concentrations, and finally reaches a plateau. A good linearity (R^2=0.976) was observed, with a detection limit (3δ/slope) of 0.76 nM, comparable to previous reports.

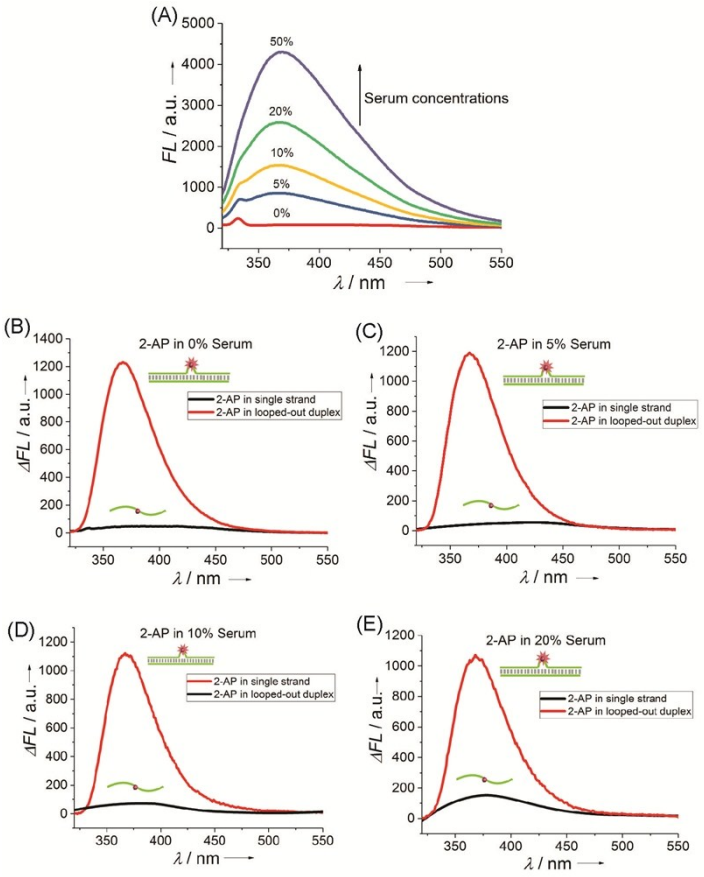

Figure S5. Effects of the serum on the fluorescence of 2-AP in the emission wavelength range from 320 nm to 550 nm (excited at 300 nm). (A) The fluorescence emission intensity increases with ascending serum concentrations. Fluorescence changes (ΔFL, deducted by the background fluorescence of serum) of 2-AP in single strand (blank line) and looped-out duplex (red line) in (A) 0%, (B) 5%, (C) 10%, (D) 20% serum.

Ⅱ. Oligonucleotide sequences

Table S3. The DNA sequences of 2-AP loop in FSG-HCR.

Lock strand	GCTTGAGATCTGAATAGAATTGCAGTCA
Control-L	TGACTGCAATTCTATGGTC
Control-R	GTCGAGCTGGTGGTTTCAGATCTCAAGC
L6	TGACTGCAATTCTATGGGAGGGT
R6	TGGGTTGGGTTTCAGATCTCAAGC
L9	TGACTGCAATTCTATGGGAGGGCGGGT
R3	TGGGTTTCAGATCTCAAGC
Hairpin 1	TGGGTGTAACTCCCTCCCACGCAGTTCTGATGGGTTGGGTCTGCGTGG GAGGGCGGGT
Hairpin 2	TGGGTTGGGTCTGCGTGGGAGGGAGTTACCGCAGACCCAACCCATCAG AATGGGAGGGT
Duplex-part-A	TCAGAAGGCAAAAAAGAGAGTAACTCCCTC
Duplex-part-B	CTGCGTGGGAGGGAGTTACTCTCTTT
HBV gene	AGTTACTCTCTTTTTTGCCTTCTGA
HIV gene	GCTAGAGATTTTCCACACTGACT
v-myc gene	GATCAGCCACCGGAACTGCA
Breast cancer gene	GAGAAACCCTATGTATGCTC
MicroDNA-21	TAGCTTATCAGACTGTTGA

The colored base indicates the 2-aminopurine substitution.

Table S4. DNA sequences of 2-AP loop in FL-HCR.

Hairpin 1	TCAGAAGGCAAAAAAGAGAGTAACTCAAAGTAGTTACTCCTTTTTTGCC
Hairpin 2	AGTTACTCTCTTTTTTGCCTTCTGAGGCAAAAAAGGAGTAACTACTTTG
HBV gene	AGTTACTCTCTTTTTTGCCTTCTGA
Mismatch 1	AGTTACTCTCTTTATTGCCTTCAGA
Mismatch 2	AGTTAGTCTCTTTATTGCCTTCAGA

The colored base indicates the 2-aminopurine substitution.

Table S5. DNA sequences of 2-AP loop in triplex study.

Single strand	TTTCTTCCCCTTTACCTCTCCCTTTTCC
Hairpin 1	CCTTTTCCCTCTCCTTTCCCCTTCTTTCGAGCAAAGAAGGGGAAAGGAGAGGGAAAAGG
Hairpin 2	CCTTTTCCCTCTCTTTCCCCTTCTTTCGAGCAAAGAAGGGGAAAGAGAGGGAAAAGG
Hairpin 3	CCTTTTCCCTCTTTTCCCCTTCTTTCGAGCAAAGAAGGGGAAAAGAGGGAAAAGG

The colored base indicates the 2-aminopurine substitution.

Ⅲ. Reference

1. J. R. Unruh, G. Gokulrangan, G. S. Wilson and C. K. Johnson, *Photochem. Photobiol.*, 2007, **81**, 682-690.
2. T. M. Nordlund, D. G. Xu and K. O. Evans, *Biochemistry*, 1993, **32**, 12090-12095.
3. L. Wang, A. K. Gaigalas, J. Blasic and M. J. Holden, *Spectrochim. Acta, Part A*, 2004, **60**, 2741-2750.
4. M. E. Sanborn, B. K. Connolly, K. Gurunathan and M. Levitus, *J. Phys. Chem. B*, 2007, **111**, 11064-11074.
5. A. Cuppoletti, Y. J. Cho, J. S. Park, C. Strassler and E. T. Kool, *Bioconjugate Chem*, 2005, **16**, 528-534.
6. S. F. Mason, *J. Chem. Soc.*, 1954, 2071.
7. S. C. Hung, R. A. Mathies and A. N. Glazer, *Anal. Biochem.*, 1998, **255**, 32-38.
8. R. B. Mujumdar, L. A. Ernst, S. R. Mujumdar, C. J. Lewis and A. S. Waggoner, *Bioconjugate Chem*, 1993, **4**, 105-111.
9. S. P. Lee, D. Porter, J. G. Chirikjian, J. R. Knutson and M. K. Han, *Anal. Biochem.*, 1994, **220**, 377-383.
10. T. Li, E. Wang and S. Dong, *J. Am. Chem. Soc.*, 2009, **131**, 15082-15083.
11. Y. J. Hu, Y. Liu, J. B. Wang, X. H. Xiao and S. S. Qu, *J. Pharm. Biomed. Anal.*, 2004, **36**, 915-919.
12. G. Weber, *Biochem. J.*, 1952, **51**, 155-167.